Research Article

Received: 8 May 2011 Revised: 31 October 2011 Accepted: 7 December 2011 Published online in Wiley Online Library: 20 February 2012

(wileyonlinelibrary.com) DOI 10.1002/pi.4163

Wavelength conversion using rare earth doped oxides in polyolefin based nanocomposite films

Abhijit Jadhav,[a] Amol Pawar,[a] Tae Ryong Hwang,[b] Jae Wook Lee,[b] Min Wook Choi,[c] Byung Kyu Kim[c] and Young Soo Kang[a]*

Abstract

Nanocomposites are a new class of polymeric materials which include organic or inorganic nano-phase materials. These nanocomposite films can show interesting properties which have many applications for wavelength conversion and energy saving. In this paper, we present polyolefin based nanocomposite films prepared using wavelength-converting red 'phosphors' such as Y_2O_3: Eu^{3+} and $LiAl_5O_8$:Fe^{3+} and blue 'phosphor' $CaMgSi_2O_6$: Eu^{2+}. The durability of the polymer chain is unaffected by incorporation of inorganic nanoparticles as there is no direct interaction between them. The addition of surfactant in the nanocomposite film helps to improve the dispersion ability of the nanoparticles and increase the flexibility of the polymer film. Wavelength-converting 'nanophosphors' incorporated in a polymer matrix help to increase the tensile strength of the film. The films show excellent wavelength conversion ability of UV light into the visible and near IR range. These nanocomposite films have great application in energy saving devices.

Supporting information may be found in the online version of this article.

Keywords: nanocomposite films; wavelength conversion; polyolefin films; inorganic phosphors; mechanical properties

INTRODUCTION

The increasing development and availability of nanomaterials have shown a variety of applications in various fields. The development of polymer nanocomposites is one of the areas of particular interest. Polymer nanocomposites are materials formed from a combination of inorganic nanomaterials and organic polymers, which show properties of both components.[1] The presence of these nanoparticles shows improvement in the elastic modulus without decreasing the elongation at break.[2–4] The basic requirement of an efficient nanocomposite film is that the base resin should have good deformation and tear resistance with sufficient rigidity. The nanophosphor should be uniformly distributed in the polymer matrix. There are various parameters which are responsible for the lifetime of a nanocomposite film such as polymer type, film type (monolayer, co-extruded multilayer), film thickness, manufacturing method, amount of filler etc.[5] Low density polyethylene (LDPE) homopolymer and ethylene–vinyl acetate copolymers (EVA) are the most commonly used thermoplastic materials for the preparation of nanocomposite films. The nanocomposite film can be prepared separately or by blending the two base resins in different proportion for the requirement of desired properties.[6]

Metal–polymer nanocomposites can be prepared by two different methods, namely *in situ*[7] and *ex situ*[8] methods. In the *in situ* methods, metal nanoparticles are synthesized inside a polymer matrix by various methods of decomposition such as thermolysis, photolysis, radiolysis etc. The metallic precursors are reduced chemically by dissolving into the polymer matrix. In the *ex situ* technique, metal nanoparticles are first synthesized by any of the known chemical methods and then dispersed in the polymer matrix.[9] In this study we prepared nanocomposite films by an *ex situ* method.

The wavelength-converting nanoparticles should have a homogeneous distribution inside the polymer matrix. The surface of the metal nanoparticles can be passivated by a monolayer of surfactant or dispersing agent. Surface passivation helps to avoid aggregation of nanoparticles and it also helps to reduce surface oxidation or contamination phenomena. Passivation of nanoparticles makes them hydrophobic and therefore they can easily be mixed with polymers.[9] The red and blue nanophosphors used in the nanocomposite films are an environmentally friendly (non-hazardous) material.

The wavelength conversion phenomenon can be carried out with the help of phosphor nanoparticles which were homogeneously distributed in the nanocomposite films. The dopant or activator in the metal oxide gets excited to a higher energy level with the absorption of UV light and it emits light of lower energy (longer wavelength) in the visible or near IR range during the relaxation process.[10] The main aim of this work was to prepare and study the properties of nanocomposite films containing wavelength-converting red and blue nanophosphors

* *Correspondence to: Young Soo Kang, Department of Chemistry, Sogang University, Seoul 121-742, Republic of Korea. E-mail: yskang@sogang.ac.kr*

a *Department of Chemistry, Sogang University, Seoul 121-742, Republic of Korea*

b *Department of Chemical and Biomolecular Engineering, Applied Rheology Laboratory, Sogang University, Seoul 121-742, Republic of Korea*

c *Department of Polymer Science and Engineering, Pusan National University, Busan 609-735, Republic of Korea*

in various proportions. Nanocomposite films of LDPE, EVA and an LDPE–EVA combination were prepared by blow extrusion as well as compression molding. For blow extrusion 3.3 wt% of red phosphor and 4.2 wt% of blue phosphor were used. For laboratory scale experiments the phosphor concentration was varied in the range 1–5 wt% of the polymer concentration.

EXPERIMENTAL

Materials

Europium doped yttrium oxide ($Y_2O_3:Eu^{3+}$)[11] synthesized by co-precipitation method and iron doped lithium aluminium oxide ($LiAl_5O_8:Fe^{3+}$) synthesized by the sol-gel method using lithium hydroxide monohydrate ($LiOH.H_2O$, 98%, Aldrich, USA), aluminium chloride ($AlCl_3$, 99.99%, Aldrich, USA) and iron chloride hexahydrate ($FeCl_3.6H_2O$, Acros Organics) as a precursor; europium doped calcium magnesium silicon oxide ($CaMgSi_2O_6:Eu^{2+}$) ($CMS:Eu^{2+}$)[10] synthesized by the co-precipitation method using calcium chloride ($CaCl_2$, 95%, Junsei Chemical Co. Ltd, Japan), magnesium chloride ($MgCl_2$ extra pure, Junsei Chemical Co. Ltd, Japan), tetraethylorthosilicate (98%, Samchung Chemicals, Korea) and europium chloride hexahydrate ($EuCl_3{\cdot}6H_2O$, 99.9% metal basis, Aldrich, USA) as a precursor; and oleic acid ($C_{18}H_{34}O_2$, Junsei Chemicals Co. Ltd, Japan), EVA (Hanhwa 2050, LG Eh 443, Korea) and linear LDPE (Hanhwa 3316, LG 0800, Korea) were used as received without further purification.

Master-batch preparation

Master-batch samples were prepared by using LDPE polymer with 3.3 wt% of $Y_2O_3:Eu^{3+}$ nanophosphor. The base resin LDPE and nanoparticles of red phosphor $Y_2O_3:Eu^{3+}$ were blended using a Buss-Kneader machine at 80 °C for 1 h. This master-batch sample was used to prepare nanocomposite films by the blow extrusion method. The nanocomposite films of LDPE–EVA-$Y_2O_3:Eu^{3+}$ (3.3 wt%) were prepared using the blow film extruder at LG Chem Ltd, Daejeon, Korea.

For laboratory scale experiments, the master-batch was prepared by the following method. Polymer base resin (1 g) was placed in a glass vial and 10 mL of cyclohexane was added to it as a solvent. The mixture was sonicated in a sonication bath at 60 °C for 2–3 h. The polymer melts and forms a clear viscous solution. Red phosphors (3 wt%), $Y_2O_3:Eu^{3+}$ and $LiAl_5O_8:Fe^{3+}$ respectively, were placed in a separate vial. Cyclohexane (10 mL) was added to it as a dispersing solvent. The mixture was sonicated at 60 °C in a sonication bath for 30 min. The well dispersed nanoparticles were added to the viscous polymer melt and sonication was continued for 2 h more in the same conditions. The excess solvent was evaporated to obtain the master-batch sample.

Nanocomposite film preparation

The nanocomposite films of LDPE–EVA (3:1 wt ratio) and LDPE–EVA-$Y_2O_3:Eu^{3+}$ (3.3 wt%) were prepared by using a blow film extruder. A regular amount of air was blown into the bubble inside the blown film under a controlled blow up ratio (BUR). Air cooling helps to bring the molten polymer to room temperature. This phenomenon is also known as temperature quenching of the film. The BUR was controlled and the thickness of the blown film was controlled between 53 and 131 μm.

The nanocomposite films were also prepared by compression molding using a Carver laboratory press at 120 °C. The LDPE–EVA film (1 g) was placed into a glass vial and 10 mL of cyclohexane was added as a solvent. Oleic acid (two to three drops) was also added as a plasticizer. The mixture was sonicated at 60 °C in a sonication bath for 2–3 h. The polymer base resin melts and forms a clear viscous solution. Various proportions of master-batch samples were placed in separate glass vials. Cyclohexane (10 mL) was added with a drop of oleic acid. The phosphor nanoparticles then get coated with oleic acid surfactant and disperse well into the cyclohexane. After 30 min sonication the dispersed nanoparticles were added to the clear viscous melt. Sonication was continued for 2 h in the same conditions. The excess solvent was evaporated and the mass remaining was used to prepare nanocomposite films by compression molding using a Carver laboratory press. The homogenized polymer resin with various proportions of red phosphor master-batch was placed over Teflon® sheets and pressed between two iron plates at 35 000 psi (2.4131×10^8 Pa), 120 °C. The nanocomposite film was quenched from 85 °C to room temperature for cooling of the molten polymer mass.

The nanocomposite films prepared by compression molding were baked in an air oven at 120 °C for 1–2 h. The heated films were immediately quenched to room temperature. The purpose of baking at high temperature is to increase the transparency of the films.

Characterization

Surface morphology was confirmed by SEM using a field emission scanning electron microscope (Hitachi S-4300) operating at an acceleration voltage of 20 kV. The percentage transmittance of the nanocomposite films at 400 nm wavelength was determined using an Agilent 8453, UV–visible spectrophotometer. Room temperature photoluminescence (PL) spectra of the nanocomposite films were measured using a Hitachi F-7000 fluorescence spectrophotometer. The phosphor materials in the nanocomposite films were excited using various wavelengths ($Y_2O_3:Eu^{3+}$ 265 nm, $LiAl_5O_8:Fe^{3+}$ 454 nm and $CMS:Eu^{2+}$ 337 nm) of a xenon lamp. Incorporation of phosphor material in the polymer matrix was also confirmed by IR spectroscopy using a Nicolate Avatar 330 FTIR instrument. The water contact angle of the nanocomposite film was measured using a Phx 300 contact angle measurement instrument. The mechanical strength of the as-prepared nanocomposite films was measured on a UTM Lloyd instrument.

RESULTS AND DISCUSSION

Morphological characterization

The nanocomposite films prepared using blow extrusion and compression molding were analyzed by SEM to evaluate the homogeneity of the added filler in the polymer matrix and to observe the nature of the film surface. Figure 1 shows SEM images of nanocomposite films prepared by co-extrusion: (A) LDPE–EVA, (B) LDPE–EVA-$Y_2O_3:Eu^{3+}$ and (C) LDPE–EVA-$Y_2O_3:Eu^{3+}$-$CMS:Eu^{2+}$. Films (D) EVA-$Y_2O_3:Eu^{3+}$, (E) EVA-$CMS:Eu^{2+}$, (F) EVA-$LiAl_5O_8:Fe^{3+}$, (G) LDPE-$Y_2O_3:Eu^{3+}$, synthesized by co-precipitation method,(H) LDPE-$CMS:Eu^{2+}$ and (I) LDPE-$LiAl_5O_8:Fe^{3+}$ were prepared using compression molding with 1 wt% of phosphor material. The films prepared using blow extrusion show a more uniform dispersion of phosphor material and higher surface smoothness, as seen in Figs 1(A)–1(C). The nanocomposite films prepared using a hot press also show a uniform dispersion of phosphor material but the surface of the film is relatively less smooth compared with the films prepared using blow extrusion. It was also observed that roughness of the film surface increases with increase in phosphor amount in the nanocomposite film.

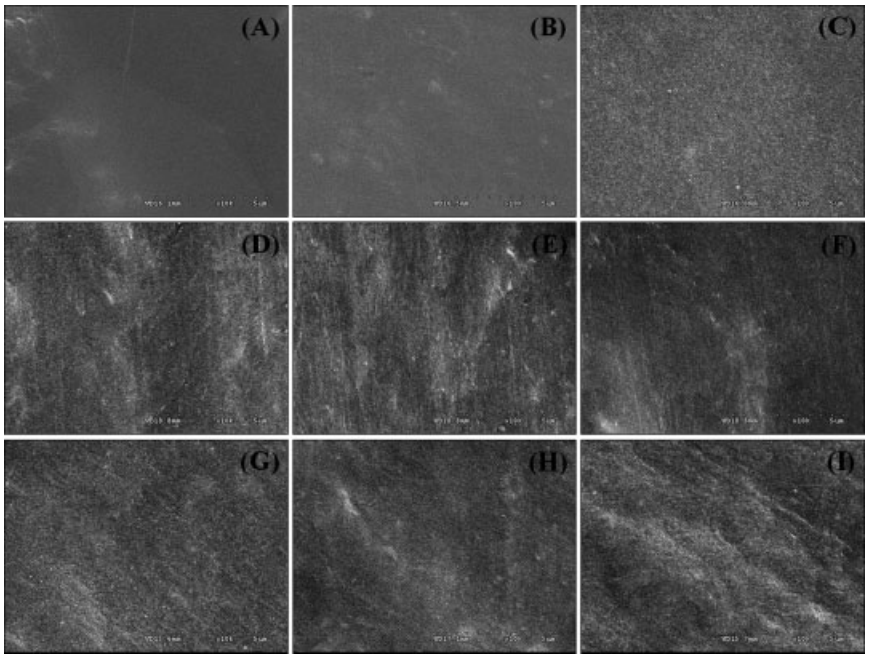

Figure 1. SEM images of nanocomposite films prepared by co-extrusion: (A) LDPE–EVA; (B) LDPE–EVA-Y_2O_3: Eu^{3+}; (C) LDPE–EVA-Y_2O_3: Eu^{3+}-CMS : Eu^{2+}. The films (D) EVA-Y_2O_3: Eu^{3+}, (E) EVA-CMS : Eu^{2+}, (F) EVA-$LiAl_5O_8$:Fe^{3+}, (G) LDPE-Y_2O_3: Eu^{3+}, synthesized by co-precipitation method, (H) LDPE-CMS : Eu^{2+} and (I) LDPE-$LiAl_5O_8$:Fe^{3+} were prepared by the hot press technique using 1 wt% of phosphor material. (Scale bar 5 μm).

UV–visible characterization

Transmission spectra of the nanocomposite films prepared by blow extrusion are shown in Fig. 2. The co-extruded film of LDPE and EVA base resin shows a maximum transmittance of 79.5% at 400 nm. Incorporation of nanoparticles of Y_2O_3: Eu^{3+} reduces this transmittance to 65.2%. The average nanoparticle size of the red phosphor material (Y_2O_3: Eu^{3+}) was around 30 nm. When blue phosphor (CMS : Eu^{2+}) nanoparticles were added to LDPE–EVA base resin, its transparency was reduced to 49.6%. The nanoparticle of blue phosphor is in an agglomerated form and non-uniformly distributed and this causes a reduction in transmittance of the nanocomposite film. When both red and blue phosphors were added to an LDPE–EVA film, the transmittance was intermediate between those of the LDPE–EVA-Y_2O_3: Eu^{3+} and LDPE–EVA-CMS : Eu^{2+} films. The combined phosphor film shows a transmittance of 61.0%.

Figure 3 shows a comparison of the transmittance spectra of EVA and LDPE nanocomposite films prepared with various amounts of $LiAl_5O_8$:Fe^{3+}, Y_2O_3: Eu^{3+} and CMS : Eu^{2+} nanophosphors. The nanocomposite films were prepared by compression molding and baked at 120 °C for 2 h in an air oven. The EVA nanocomposite film prepared with 1 wt% of phosphor shows a maximum transmittance of 82.4% for $LiAl_5O_8$:Fe^{3+}, 78.4% for Y_2O_3: Eu^{3+} and 71.0% for CMS : Eu^{2+}, respectively. In the case of LDPE nanocomposite films, the transmittance obtained with 1 wt% of phosphor was 19.2% for $LiAl_5O_8$:Fe^{3+}, 56.7% for Y_2O_3: Eu^{3+} and 23.7% for CMS : Eu^{2+}, respectively. The transmittance of the films decreases with increasing phosphor concentration. The transparency of the nanocomposite films prepared using EVA is higher than that of LDPE polymer as EVA copolymers are transparent to visible light and allow all the wavelengths essential for photosynthesis to pass through.[12] Unlike EVA polymer LDPE does not show good transparency to visible light. Hence the nanocomposite films prepared using LDPE show less transparency.

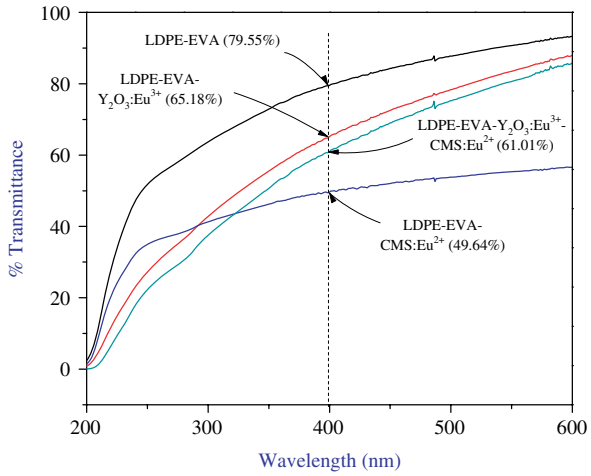

Figure 2. Per cent transmittance at 400 nm of nanocomposite films prepared by LDPE-EVA co-extrusion with 3.3 wt% of red phosphor (Y_2O_3: Eu^{3+}) and 4.2 wt% of blue phosphor (CMS : Eu^{2+}), respectively. The nanocomposite films were prepared by co-extrusion.

Transparency of a polymer film depends mainly on the nature of the polymeric material, i.e. amorphous or crystalline. Every polymer contains regions of crystalline as well as amorphous parts known as domains. A polymer cannot be 100% amorphous or crystalline in nature. Thus, if a polymer has more amorphous domains, it shows higher transparency. The incident light shows less deviation when it passes through an amorphous region. Similarly, if a polymer has more crystalline domains then the incident light will show less transparency. The transparency of a polymer film also depends on the homogeneous distribution of nanoparticles in the polymer matrix. For a homogeneous distribution of phosphor material, the nanoparticles should have

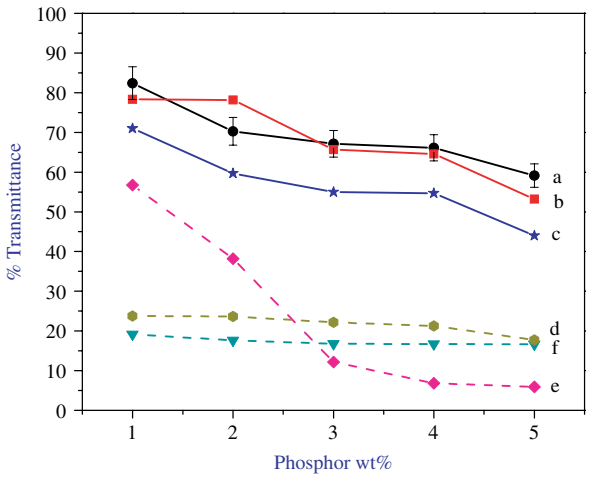

Figure 3. Transmittance at 400 nm of nanocomposite films prepared by compression molding of (a) EVA-$LiAl_5O_8$:Fe^{3+}, (b) EVA-Y_2O_3: Eu^{3+}, (c) EVA-CMS : Eu^{2+}, (d) LDPE-$LiAl_5O_8$:Fe^{3+}, (e) LDPE-Y_2O_3: Eu^{3+} and (f) LDPE-CMS : Eu^{2+}, using 1–5 wt% of $LiAl_5O_8$:Fe^{3+}, Y_2O_3: Eu^{3+} and CMS : Eu^{2+} nanophosphors, respectively.

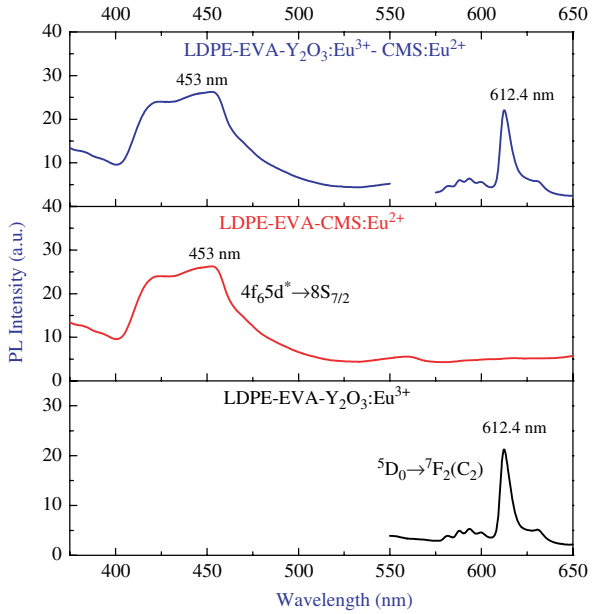

Figure 4. Room temperature PL spectrum of the nanocomposite film prepared by LDPE–EVA co-extrusion with 3.3 wt% of red phosphor (Y_2O_3: Eu^{3+}), 4.2 wt% of blue phosphor (CMS : Eu^{2+}) and a combination of the two phosphors. The nanocomposite films were prepared by co-extrusion.

a narrow size distribution. The surface of the nanoparticles should be passivated for homogeneous distribution and also to avoid aggregation. The aggregation of nanoparticles can reduce the transparency of a film as the incident light will be absorbed and scattered by aggregated nanoparticles. In our case we have used oleic acid for passivation of the nanoparticle surface. Uniformly distributed nanoparticles will have a higher surface area in the polymer matrix. As a higher number of particles is going to interact with the incident UV light, wavelength conversion efficiency of the nanocomposite film increases. In this study we found that, when the phosphor concentration in the nanocomposite film increases, the transparency of the composite film decreases. This is due to incorporation of a higher amount of inorganic phosphor material; the distance between intermolecular polymer chains reduces and this leads to lower transparency of the film.

Optical properties

The conversion of absorbed UV light into the visible or near IR range was confirmed by measurement of the PL spectra of the nanocomposite films prepared by blow extrusion as well as compression molding. Figure 4 shows the room temperature PL spectrum of the nanocomposite film prepared by using LDPE–EVA co-extrusion with 3.3 wt% of Y_2O_3: Eu^{3+}, 4.2 wt% CMS : Eu^{2+} and a combination of both phosphors. The nanoparticles of Y_2O_3: Eu^{3+} absorb UV light at 265 nm and show emission in the red region at 612.4 nm. The emission peaks of the red and blue phosphors with corresponding electronic transitions are given in Table 1. This red emission confirms that the phosphor material in the nanocomposite film absorbs high energy UV light and converts it into lower energy red light. The blue phosphor in the film absorbs UV light at 337 nm wavelength and emits blue light at 453 nm wavelength. The most intense peak at 453 nm was observed due to the $^4f^6(^5D^*)$-$^8S_{7/2}$ transition. In the Eu^{2+} state, electrons are excited from $^8S_{7/2}$ (ground state) to $4f^65d$ (excited state) at 337 nm wavelength and get relaxed as $4f^65d \rightarrow 4f^65d^*$. This relaxed electron de-excites as $4f^65d^* \rightarrow ^8S_{7/2}$ with blue emission at 453 nm. The red phosphor (Y_2O_3: Eu^{3+}) in the film gets excited at 265 nm while the blue phosphor (CMS : Eu^{2+}) gets excited at 337 nm of the xenon lamp. The red and blue phosphors show no interference with each other in the PL spectra.

Table 1. Electronic transition during PL excitation and emission of LDPE–EVA-Y_2O_3: Eu^{3+} and LDPE–EVA-CMS : Eu^{2+} nanocomposite films

Film type	λ_{exc} (nm)	λ_{emi} (nm)	Electronic transition
LDPE–EVA-Y_2O_3: Eu^{3+}	265	630.6	$^5D_0 \rightarrow ^7F_2$ (C_2)
		612.4	$^5D_0 \rightarrow ^7F_2$ (C_2)
		599.6	$^5D_0 \rightarrow ^7F_1$ ($C_2 + S_6$)
		593.4	
		587.8	
		581.4	$^5D_0 \rightarrow ^7F_0$ (C_2)
LDPE–EVA-CMS : Eu^{2+}	337	453	$^4f^6(5D^*) \rightarrow ^8S_{7/2}$

The PL spectra of nanocomposite films prepared by compression molding using EVA and LDPE polymers with various amounts of red phosphors ($LiAl_5O_8$:Fe^{3+} and Y_2O_3: Eu^{3+}) and blue phosphor (CMS : Eu^{2+}) are shown in Fig. 5. In the case of EVA nanocomposite films, 4 wt% $LiAl_5O_8$:Fe^{3+}, 3 wt% Y_2O_3: Eu^{3+} and 5 wt% CMS : Eu^{2+} gave maximum luminescence intensity. For LDPE nanocomposite films, 4 wt% of $LiAl_5O_8$:Fe^{3+} and Y_2O_3: Eu^{3+}, respectively, and 5 wt% of CMS : Eu^{2+} gave maximum luminescence intensity. Above the optimum concentration the intensity of the emission peak decreases. In the case of nanocomposite films, the emission intensity depends mainly upon the amount of phosphor nanoparticles present in the measured area of the film. As the phosphor concentration increases, the number of excited electrons will also increase and excited electrons transfer their energy to neighboring electrons by quenching during the relaxation process. Thus the intensity of the emission peak decreases with increase in phosphor concentration above

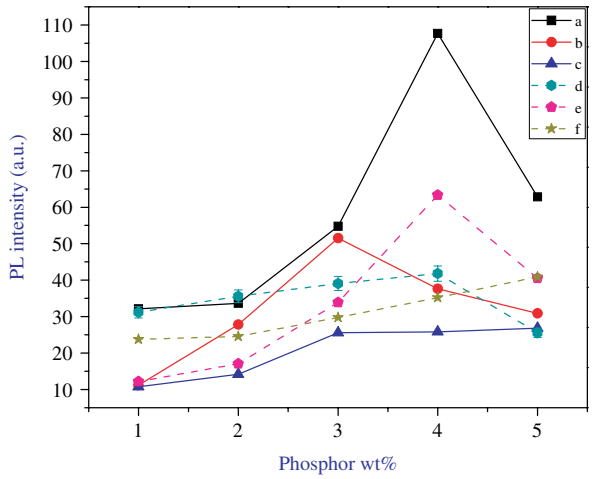

Figure 5. Comparison of room temperature PL intensity of the nanocomposite film prepared using (a) EVA-$LiAl_5O_8$:Fe^{3+}, (b) EVA-Y_2O_3: Eu^{3+}, (c) EVA-CMS : Eu^{2+}, (d) LDPE-$LiAl_5O_8$:Fe^{3+}, (e) LDPE-Y_2O_3: Eu^{3+} and (f) LDPE-CMS : Eu^{2+}, respectively, by compression molding with 1–5 wt% of $LiAl_5O_8$:Fe^{3+} (λ_{exc} = 454 nm), Y_2O_3: Eu^{3+} (λ_{exc} = 265 nm) and CMS : Eu^{2+} (λ_{exc} = 337 nm) nanophosphors.

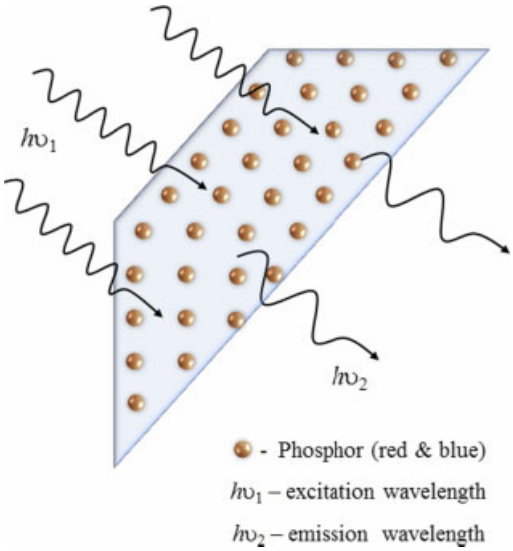

Figure 6. Schematic representation of nanocomposite films for wavelength conversion applications.

a certain limit. In EVA and LDPE nanocomposite films prepared using red phosphors, Fe^{3+} in $LiAl_5O_8$ gets excited at 454 nm and emits intense red light at 677 nm and Eu^{3+} in Y_2O_3 gets excited at 265 nm and emits red light at 612.4 nm. The blue phosphor in the nanocomposite material absorbs UV light at 337 nm and emits blue light at 453 nm. The PL spectra of EVA and LDPE nanocomposite films are shown in the supporting information (Figs S3–S8).

Figure 6 gives a schematic representation of a nanocomposite film for wavelength conversion applications. The homogeneously distributed nanoparticles of red and blue phosphor materials help to convert wavelength of higher energy ($h\nu_1$) to wavelength of lower energy ($h\nu_2$). This converted wavelength is absorbed by chlorophyll, present in plant leaves, for the process of photosynthesis. Addition of phosphor nanoparticles to the polymer matrix reduces its transparency to visible light. The phosphor material in the nanocomposite film helps to block radiation in the UV range and shows transmittance to light in visible range (400–600 nm). Wavelength-converting materials have several parameters of interest such as the absorption wavelength, the emission wavelength and the quantum/conversion efficiency. Wavelength conversion efficiency of a material can be estimated by measuring the ratio of the number of photons absorbed to the number of photons emitted. The ability of a phosphor material to convert short wavelength light to longer wavelength light is determined by two main factors, i.e. the external quantum efficiency and the inherent quantum mechanical energy loss occurring during the wavelength conversion process, as explained by Schubert:[11–13]

$$n = \frac{\text{number of photons emitted into free space by } \lambda\text{-converter per second}}{\text{number of photons absorbed by } \lambda\text{-converter per second}} \quad (1)$$

The inherent wavelength conversion loss occurring during conversion of a photon of wavelength λ_1 to a photon of wavelength λ_2 is

$$\Delta E = h\nu_1 - h\nu_2 = \frac{hc}{\lambda_1} - \frac{hc}{\lambda_2} \quad (2)$$

Thus the wavelength conversion efficiency is given by

$$\eta_{\lambda}\text{-conversion} = \frac{h\nu_2}{h\nu_1} = \frac{\lambda_1}{\lambda_2} \quad (3)$$

Here, λ_1 is the wavelength of the photons absorbed by the phosphor and λ_2 is the wavelength of the photons emitted by the phosphor.

Fourier transform IR (FTIR) characterization

IR spectra of the nanocomposite film were measured to identify the incorporation of nanophosphors in the polymer matrix. Figure 7 shows a comparison of FTIR spectra of blow extrusion films prepared using LDPE–EVA polymers with incorporation of red phosphor (Y_2O_3: Eu^{3+}) and blue phosphor (CMS : Eu^{2+}). The peak at 728 cm^{-1} represents bonds due to C–H rocking. The peaks at 1236, 1461.85 and 1739.56 cm^{-1} correspond to C–H bending while the peaks at 2894.77 and 3606.41 cm^{-1} correspond to C–H stretch and O–H stretch, respectively. The peak due to metal–oxygen bonding appears between 400 and 600 cm^{-1}. The incorporation of oxide material (red and blue phosphors) in the polymer matrix is confirmed with these peaks. Comparison of the FTIR spectra of nanocomposite films prepared by compression molding using EVA and LDPE polymers with 5 wt% of red and blue phosphors is shown in the supporting information (Figs S1 and S2). It was observed that the nanocomposite films showed peaks of both polymer base resin and incorporated nanoparticles of red and blue phosphors. The incorporation of wavelength converting nanophosphor does not make any change in the peaks of polymer sample. Thus it was confirmed that inorganic oxide nanoparticles are homogeneously dispersed in the polymer matrix and have no interaction with the polymer molecules.

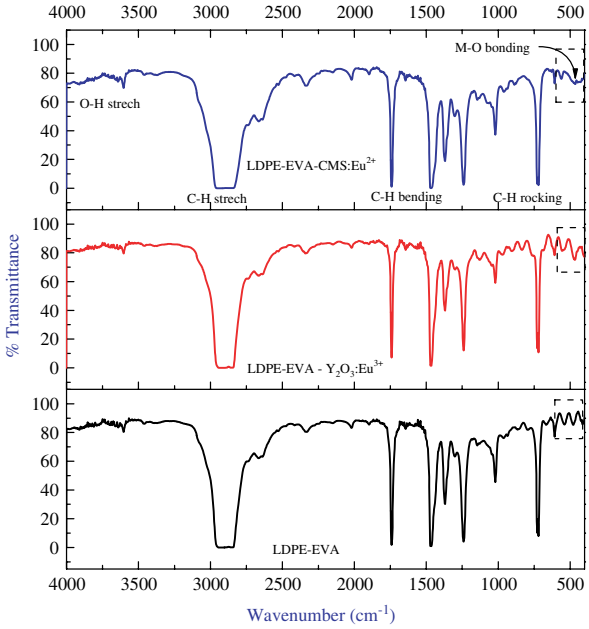

Figure 7. FTIR spectra of nanocomposite films prepared by co-extrusion of LDPE–EVA base resin, LDPE–EVA with 3.3 wt% of red phosphor (Y_2O_3: Eu^{3+}) and LDPE–EVA with 4.2 wt% of blue phosphor (CMS : Eu^{2+}), respectively.

Mechanical characterization

All nanocomposite films were mechanically characterized by measurement of thickness, strain and stress at break. The data for the mechanical properties of the nanocomposite films is presented in Table 2. The tensile strength of a polymer is the maximum load it can sustain before permanent deformation. It depends mostly on various factors such as molecular structure, chain length, surfactant content and amount of filler. In the case of nanocomposites the strength of a polymer will only be affected by the amount of filler (inorganic nanoparticles) in it. As the amount of filler increases in a polymer matrix, the free movement of molecular chains will be restricted by the presence of the filler. Thus the mechanical strength will be increased in proportion to the amount of nanophosphor added. Graphs of the tensile strength of the nanocomposite films prepared by the compression molding method are shown in Fig. 8. It is observed that the strength of the nanocomposite film increases with incorporation of nanoparticles into the polymer matrix. A similar phenomenon was observed in the case of nanocomposite films prepared by the compression molding method. The tensile strength of a polymer nanocomposite film increases with increase in the proportion of nanophosphor in it. A homogeneous distribution of nanoparticles in the polymer matrix is also necessary to prepare a nanocomposite film with higher mechanical strength.

Contact angle

Table 3 shows the surface energies and water contact angles of nanocomposite films prepared using EVA-Y_2O_3: Eu^{3+}, LDPE-Y_2O_3: Eu^{3+} and EVA-CMS : Eu^{2+}, respectively. The water contact angles of the nanocomposite films were measured in order to evaluate the modification in surface properties due to the presence of nanophosphor materials. Contact angle measurement can determine the surface energy γ of a solid surface. The surface energy is the energy per unit area of an exposed surface of a liquid,

Table 2. Mechanical properties of nanocomposite films prepared using blow extrusion and compression molding

Sample	Thickness (mm)	% Strain at maximum load	% Strain at break	Stress at break (MPa)
LDPE–EVA	59	120.18	126.09	15.68
LDPE–EVA-RED	53	122.99	131.13	14.89
LDPE–EVA-BLUE	131	269.83	224.11	13.39
EVA-RED (5 wt%)	129	56.61	610.33	6.14
LDPE-RED (5 wt%)	116	422.45	422.25	10.86
EVA-BLUE (5 wt%)	136	500.68	391.78	6.71
LDPE-BLUE (5 wt%)	146	41.92	135.36	7.69

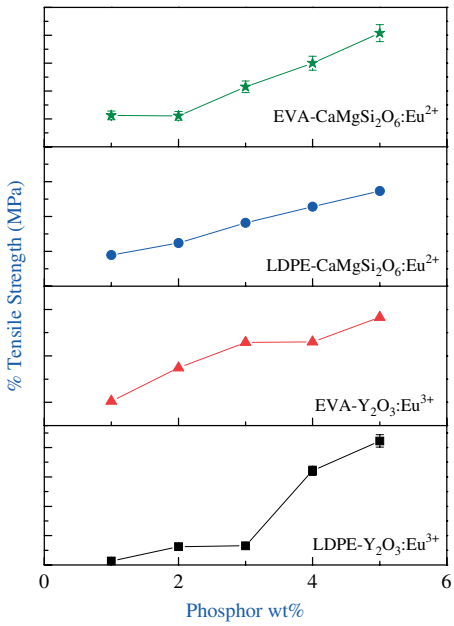

Figure 8. % (percentage) tensile strength of the nanocomposite films prepared by using LDPE and EVA base resin separately with 1–5 wt% of red (Y_2O_3: Eu^{3+}) and blue (CMS : Eu^{2+}) phosphors. The nanocomposite films were prepared by the compression molding method.

and is generally greater than the surface tension, which equals the free energy per unit surface. Surface energy quantifies the disruption of the intermolecular bonds that occurs when a surface is created.

The surface energy of a material can be measured using the Owens–Wendt surface energy calculation

$$(1 + \cos\theta_i)\gamma_{LS} = 2(\gamma_L^D \gamma_S^D)^{0.5} + 2(\gamma_L^P \gamma_S^P)^{0.5} \quad (4)$$

where θ is the contact angle and the labels L, S, D and P refer to the liquid surface, the solid surface, the London dispersion force and the polar dispersion force respectively. Kennedy *et al.* and Roberson *et al.*[14,15] converted water contact angle to surface energy using the equation

$$\text{surface energy} = 74.5 - 0.372x - 0.00181x^2 \quad (5)$$

where x is the water contact angle in degrees.

For a given material, the surface energy is inversely proportional to its water contact angle. In the case of nanocomposite films, as

Table 3. Water contact angles and surface energies of nanocomposite films prepared using red (Y_2O_3: Eu^{3+}) and blue (CMS : Eu^{2+}) nanophosphors

	EVA-Y_2O_3: Eu^{3+}		LDPE-Y_2O_3: Eu^{3+}		EVA-CMS : Eu^{2+}	
Phosphor (wt%)	Contact angle (°)	Surface energy (dyn cm^{-1})	Contact angle (°)	Surface energy (dyn cm^{-1})	Contact angle (°)	Surface energy (dyn cm^{-1})
0	78.06	34.433	84.25	30.312	78.06	34.433
1	77.66	34.694	82.89	31.229	77.38	34.872
2	76.78	35.268	79.75	33.321	75.97	35.792
3	76.11	35.702	77.08	35.072	74.80	36.871
4	75.46	36.122	76.01	35.767	72.64	37.920
5	75.32	36.213	75.41	36.155	66.26	41.900

Error bar (deviation in contact angle measurement): ± 2°.

we increase the concentration of nanophosphors in the polymer matrix, the surface roughness of the film increases. The rough surface decreases the contact angle and increases the surface energy as a large area of the film is in contact with water. To be an effective nanocomposite film, the nanoparticles of wavelength-converting materials should have a homogeneous distribution in the polymer matrix. Homogeneously distributed nanoparticles give a smooth surface to the nanocomposite film, which is more hydrophobic. An uneven distribution of nanoparticles or aggregation leads to a rough surface and also reduces the water contact angle of the nanocomposite film. The contact angle of a polymer film also depends upon the amount of filler used in the film. In our case the contact angle of the nanocomposite film decreases with increase in the proportion of nanophosphor material in the polymer film. From Table 3, it is observed that as the amount of nanophosphor increases, the water contact angle decreases with increase in surface energy of the film. The data also indicate that the surface roughness of the film is increased with increase in the amount of nanophosphor in the polymer film.

The nanocomposite films prepared by blow extrusion were used as the cover of a greenhouse where various kinds of agricultural crops were grown. The results of growth of tomato plants and melon plants in various film environments are presented in Table 4. The results of as prepared nanocomposite films were compared with commercially available film EF221. In the case of tomato plants, the weight of fruit was increased with incorporation of wavelength-converting nanophosphors. The combination of red and blue nanophosphor film shows a maximum weight of tomato fruit with increase in the number of seeds per week. Similarly with melon fruit, the combination of red and blue nanophosphor film gives maximum weight of melons with increase in sugar content of the fruit. Thus it was observed that wavelength-converting nanoparticles helps to convert UV light into the visible and far IR range which can be helpful for increasing photosynthetic activities in plants. The prepared nanocomposite films help to enhance quality and quantity of crops in a greenhouse environment.

Table 4. Photoelectric exchange growth characteristics of tomato and melon plants according to film type

	Tomato		Melon	
Film type	Weight (kg $week^{-1}$)	No. of seeds per week	Weight of fruit (kg)	Sugar content in °Bx = 1 g sucrose in 100 g of solution
PE	13.4	2.40	1.48	13.8
Red	13.6	2.68	1.56	14.2
Blue	14.6	2.87	1.45	13.9
Red + blue	14.8	2.46	1.62	14.3
EF221	14.4	2.67	1.52	13.7

EF221 is a commercial greenhouse film from Hyundai Petrochemical with 3 wt% EVA.

CONCLUSION

Nanocomposite films were prepared by blow extrusion using co-extrusion of LDPE and EVA base resins, and separately by compression molding. Addition of oleic acid helps to achieve a homogeneous nanoparticle distribution inside the polymer matrix. Transparency of the nanocomposite films increases greatly after baking and quenching. A uniform distribution of wavelength-converting nanoparticles plays an important role in increasing the transmittance of the nanocomposite films. The properties of the polymer films remained unaffected as there is no interaction between the inorganic nanoparticles and the polymer chains. The nanocomposite films show excellent characteristics of converting UV light into the visible or near IR range.

ACKNOWLEDGEMENTS

The authors thank Mr Chang Hwan Jang (LG Chem Ltd, Daejeon, Korea) for his help in preparation of nanocomposite films by the blow extrusion method. This work was financially supported by Energy Technology Research and Development 2008-2010. This work was also supported by the Basic Science Research Program through a National Research Foundation of Korea (NRF) grant funded from the Ministry of Education, Science and Technology (MEST) of Korea for the Center for Next Generation Dye-sensitized Solar Cells (No. 2010-0001842).

SUPPORTING INFORMATION

Supporting information may be found in the online version of this article.

REFERENCES

1 Ashton HC, *Polymer Nanocomposites Handbook*, CRC Press, Boca Raton, Florida, p. 22 (2010).
2 Vaia RA and Giannellis EP, *Macromolecules* **30**:7990 (1997).
3 Liu LM, Qi ZN and Zhu XG, *J Appl Polym Sci* **71**:1133 (1999).

4 Kato M, Usuki A and Okada A, *J Appl Polym Sci* **66**:1781 (1997).
5 Halim Hamid S, *Handbook of Polymer Degradation*, 2nd edition, Marcel Dekker, New York (NY), p. 40 (2000).
6 Scaffaro R, Botta L and Mantia FPL, *Macromol. Mater. Eng.* **294**:445–454 (2009).
7 Yang J, Hasell T, Wang W and Howdle SM, *Eur Polym J* **44**:1331–1336 (2008).
8 Brust M, Walker M, Bethell D, Schiffrin DJ and Whyman R, *J Chem Soc Chem Commun* **15**:801–802 (1994).
9 Carotenuto C, Nicolais L, Martorana B and Perlo P, *Metal–Polymer Nanocomposites*, John Wiley & Sons, Hoboken, NJ, p. 156 (2005).
10 Pawar AU, Jadhav AP, Pal U, Kim BK and Kang YS, *J Lumin* **132**:659–664 (2012).
11 Jadhav AP, Pawar A, Kim CW, Cha HG, Pal U and Kang YS, *J Phys Chem C* **113**:16652–16657 (2009).
12 Halim Hamid S, *Handbook of Polymer Degradation*, 2nd edition, Marcel Dekker, New York (NY), p. 41 (2000).
13 Schubert EF, *Light-Emitting Diodes*, 2nd edition, Cambridge University Press, New York, p. 347 (2006).
14 Kennedy SB, Washburn NR, Simon Jr CG and Amis EJ, *Biomaterials* **27**:3817–3824 (2006).
15 Roberson SV, Fahey AJ, Sehgal A and Karim A, *Appl Sur Sci* **200**:150–164 (2002).

